Plant Ecol (2018) 219:1259–1267
https://doi.org/10.1007/s11258-018-0876-5

Projected drought effects on the demography of Ashe juniper populations inferred from remote measurements of tree canopies

H. Wayne Polley · Daniel M. Johnson · Robert B. Jackson

Received: 4 June 2018 / Accepted: 20 August 2018 / Published online: 24 August 2018

Abstract Tree mortality from drought is anticipated to increase as climate change promotes more frequent or severe water limitation. Ecosystem impacts of woody mortality depend on both the number and sizes of trees that die, but a limited capacity to predict mortality risk for individual trees hinders the capacity to forecast drought effects on tree population demography and ecosystem processes. We remotely measured leaf area of living Ashe juniper trees at three savanna sites in central Texas, USA to characterize the frequency-size distribution (FSD) of juniper populations and evaluate mortality risk from drought as a function of tree size. Mortality risk of individuals was assessed from the deviation in leaf area per tree from that of a similarly sized individual with near maximal leaf area using correlations among leaf area, growth rate, and mortality measured during a prior drought. We found that the FSD of juniper trees is bell-shaped at each site. Mortality risk from drought exceeded 25% of emergent (> 4 m height) trees in savanna juniper populations, but was highest for largest trees. Mortality risk was greatest at a grazed savanna, exceeding 50% of trees with projected canopy area > 20 m^2. Results imply that severe drought could kill a large fraction (18–85%) of intermediate- to large-sized Ashe juniper trees in central Texas savannas. Our analysis demonstrates a novel use of remote measurements of canopy foliation to link mortality risk from drought to the demography of Ashe juniper populations through properties of individual trees.

Keywords Canopy area · Climate change · Leaf area · Remote sensing · Savanna · Tree mortality

Communicated by Carissa Lyn Wonkka.

H. W. Polley (✉)
USDA–Agricultural Research Service, Grassland, Soil & Water Research Laboratory, Temple, TX 76502, USA
e-mail: wayne.polley@ars.usda.gov

D. M. Johnson
Warnell School of Forestry and Natural Resources, University of Georgia, Athens, GA 30602, USA

R. B. Jackson
Department of Earth System Science, Woods Institute for the Environment and Precourt Institute for Energy, Stanford University, Stanford, CA 94305, USA

Introduction

Droughts are killing an increasing number of trees worldwide (Allen et al. 2010; Carnicer et al. 2011; Peng et al. 2011) and are anticipated to become more frequent or severe as the result of climate change (IPCC 2013; Trenberth et al. 2014). Ecosystem impacts of extensive woody mortality include reductions in carbon sequestration (Huang et al. 2010; Michaelian et al. 2011) and changes in hydrology (Adams et al. 2012; Guardiola-Claramonte et al.

2011), but depend on both the number and sizes of trees that die (Anderegg et al. 2016; Pfeifer et al. 2011). Tree death may have greatest short-term ecosystem impact when mortality is concentrated among large individuals because large trees exert disproportionate control on ecosystem functioning (Belsky et al. 1989; Stephenson et al. 2014).

Several studies had demonstrated that drought effects on tree mortality vary with tree size (effects are size-discriminate). Drought often kills larger, presumably older, trees that have been growing most slowly (Bennett et al. 2015; Floyd et al. 2009; Moore et al. 2016; Mueller et al. 2005; Ogle et al. 2000; Suarez et al. 2005). High mortality among large overstory trees will skew the frequency-size distribution (FSD) of woody populations toward smaller individuals with possible ecological consequences that are disproportionate to the fraction of the trees that succumb to drought (Bennett et al. 2015; Pfeifer et al. 2011; Stephenson et al. 2014). Death of large trees is anticipated to have a particularly large impact in open woodlands and savannas where emergent trees are embedded in a matrix of herbaceous vegetation and are relatively insensitive to fire or competition that kill small trees (Noel and Fowler 2007; Taylor et al. 2012). By contrast, mortality that is size-indiscriminate would reduce tree number, but not change the FSD of tree populations.

The anticipated increase in drought frequency or severity emphasizes the ecological relevance of developing methods to predict drought effects on both the numbers and size distribution of individuals in woody populations. Methods that link disturbance effects to properties of individual trees may be required to accurately predict drought-caused shifts in the population structure of woody vegetation, particularly at relatively fine spatial scales.

The historic drought of 2011–2013 in central Texas, USA caused extensive and widespread mortality of woody species (Johnson et al. 2018; Moore et al. 2016; Schwantes et al. 2016, 2017). The 2011–2013 drought was the most severe since the initiation of records in 1895 (Hoerling et al. 2013). It is estimated that 300 million trees in Texas died during the drought, 100 million of which were in the central part of the state (Moore et al. 2016; Schwantes et al. 2017). Woody mortality was linked to hydraulic failure belowground (Johnson et al. 2018). Mortality was particularly high in Ashe juniper (*Juniperus ashei* J. Buchholz; Schwantes et al. 2017) trees, which experienced 27% canopy dieback in the Edwards Plateau region in west-central Texas (Johnson et al. 2018). Ashe juniper is a keystone woody species in the Edward Plateau region, having increased in density in areas previously characterized as live oak savannas (Taylor et al. 2012) as the result of overgrazing or fire suppression (Riskind and Diamond 1988; Smeins and Merrill 1988). Density and cover of juniper regulate hydrology and livestock productivity (Allred et al. 2012; Taucer et al. 2008), among other ecosystem processes.

We demonstrated previously that Ashe juniper trees that grew slowly prior to the 2011–2013 drought were disproportionately likely to die during or following drought (Polley et al. 2016). Slow growth, in turn, was linked to sparse foliation of tree canopies, measured as the reduction in tree leaf area (LA) from the LA of a similarly sized individual growing on deep soil and presumed to have experienced minimal water limitation. In this study, we remotely measured LA per unit of canopy area of living Ashe juniper trees at three savanna sites to characterize the FSD of emergent (> 4 m height and taller than individuals of any shrub species) trees in juniper populations and evaluate mortality risk from drought as a function of tree size. We predicted that (1) emergent trees of Ashe juniper would exhibit a 'bell-shaped' FSD, indicative of savanna populations in which mortality rate is greater among small and large individuals than trees of intermediate size, and (2) mortality risk from severe drought would exceed 20% of savanna populations and be concentrated among largest trees, consistent with trends documented following the 2011–2013 drought (Johnson et al. 2018; Polley et al. 2016; Schwantes et al. 2016, 2017).

Materials and methods

Study sites

During July–October 2016 and July–September 2017, we measured the size and LA of living Ashe juniper trees in savanna settings at three locations in central Texas, USA: Colorado Bend State Park (31°05′N, 98°48′W) located near the city of Lampasas; an old-field site in the city of Temple (31°10′N, 97°34′W); and a cattle ranch located near the town of Moffat (31°20′N, 97°47′W). Sites were chosen to be

representative of differences in soils and management in central Texas. Colorado Bend Park and Moffat ranch are characterized by shallow clay loam soils underlain by fractured limestone with 1–5% slopes (Schwinning 2008). The old-field site in Temple is on deep clay soil. Annual precipitation averages 755 mm (50-year record) at Colorado Bend and 875 mm (91-year record) at Temple and Moffat. Management differs among the three locations. Moffat Ranch is grazed by cattle. The Colorado Bend savanna site is burned during summer at approximately 6-year intervals. The Temple old-field site has not been disturbed for $>$ 25 years.

We sampled living juniper trees growing as isolated individuals or along the margins of clusters of 2–4 trees interspersed among herbaceous vegetation (in a savanna setting), trees for which we could clearly discern aerial canopy projection from directly above individuals. Ashe juniper individuals branch near the plant base creating trees that are rounded in shape. Our objective was to measure the aerial canopy projection (size) and leaf area index (LAI) of a representative sample of juniper trees at each location. To that end, we sampled every living juniper tree encountered along and within 25 m of transects at Moffat and Colorado Bend. We sampled along parallel transects, each approximately 0.5 km in length, that were spaced 100 m apart at the Moffat site. Juniper savanna at Colorado Bend was largely restricted to the north and western boundary of the Park. At Colorado Bend, we sampled along an approximately 5.5 km transect that paralleled the north and western Park boundary. We exhaustively sampled juniper trees growing in savanna setting at the small (4.7 ha) old-field site in Temple.

Remote measurements of tree size and leaf area

For each living tree with LAI $>$ 2 (approximately 4 m height) that was encountered, we measured both LAI and projected canopy area (CA), the latter defined as the surface area projected by the tree canopy. LAI and CA per tree were derived from measurements from an unmanned aerial vehicle (UAV) platform (S1000; DJI; Shenzhen, China). LAI per tree was calculated from measurements of the spectral signature of reflected radiation with an ASD HandHeld2 Pro spectroradiometer (spectral range of 350–1070 nm; ASD Inc., Boulder, CO, USA) that was mounted beneath the UAV. We measured reflectance by flying the rotary-wing UAV directly above each tree. Feedback from a video monitor attached to the UAV was used to lower the UAV to the height at which the full canopy of the target tree was first included in the 25° field of view (FOV) of the spectroradiometer. Three measurements of reflectance per tree then were taken from this stationary position and subsequently averaged. Height of the UAV was measured using an on-board altimeter. The UAV then was lowered beside the target tree to the height at which the tree canopy was widest. UAV height above the soil surface then was recorded. Maximum canopy diameter of each tree (m) was calculated from the footprint projected by a 25° angle at distance equal to the difference between the UAV height at which the full canopy of the target tree was first included in the spectroradiometer FOV and the widest canopy dimension was encountered. Reflectance was measured on cloudless days within 2 h of solar noon. Measurements were referenced to a standard barium sulfate panel at $\sim$ 15-min intervals to maintain consistency in observations. CA was calculated from maximum canopy diameter by assuming that the canopy was circular in shape. Leaf area per tree (LA) was calculated by multiplying LAI by CA.

Calculation of LAI

Partial least squares regression (PLSR) analysis was used to calculate tree LAI from measurements of spectral reflectance. PLSR uses the continuous spectrum of reflectance measurements in prediction and accommodates collinearity among spectral signals by reducing the number of predictive signals to a smaller set of uncorrelated components or latent variables that explain variation in both response and predictor variables (Wold et al. 1984). Prior to PLSR analysis, we averaged reflectance measurements from each tree over 5-nm wavebands, beginning at the 661–665 nm band and ending at 756–760 nm, and 10-nm wavebands over the remainder of the 350–1070 nm spectrum, resulting in a total of 82 wavebands. Reflectance data for the 82 wavebands per tree then were scaled 0–1 (Brightness normalization; Feilhauer et al. 2010). A predictive PLSR equation for LAI was developed using measurements of LAI and spectral reflectance on 53 additional (calibration) trees that spanned the range of mature tree sizes encountered in savannas (LAI range 2.0–5.8). LAI was derived for each of the 53 calibration individuals by measuring tree

interception of photosynthetically active radiation using a SunScan canopy analysis system (Delta-T Devices, Ltd., Burwell, Cambridge, UK). CA of calibration trees and of individuals encountered in savannas for which remote measurement of LAI was not feasible was calculated from physical measurements of maximum canopy diameter. Of trees on which we calculated CA from physical measurements of canopy diameter (28 and 17 trees at Moffat and Temple, respectively), most were too small to reliably estimate LAI from canopy reflectance. We physically measured a much larger cohort of trees (460) at Colorado Bend, with measured trees distributed across size classes encountered. We constructed size (CA)-frequency distributions for juniper trees from each location using size-class bins of 10 m^2 CA.

The optimal number of spectral latent variables required to predict LAI was determined using a "split-sample" cross-validation procedure in PLSR. A PLSR model was fit to a data set composed of data from every 7th tree in the list of 53 calibration trees beginning with the first tree in the list, while minimizing the prediction error for unfitted data. The process was repeated iteratively by beginning split-sample data sets with data from each successive tree in the list of 53. We chose the PLSR model with > 1 latent variable that produced the first minimum in residuals from LAI predictions of unfitted data (root mean predicted residual sum of squares; PRESS). PLSR was fit using SAS 9.4.

Mortality risk

We estimated drought mortality risk or vulnerability per savanna tree sampled using the difference between the LA calculated using spectral reflectance and the 'maximum' LA value for a tree of the same CA. 'Maximum' values of LA were considered as equal to values at the 90th percentile of a quantile regression fit to the linear relationship between LA and CA for all savanna trees combined (= LA_{90}; Cade and Noon 2003). We standardized LA deviation from maximum for tree size by subtracting observed LA from the maximum LA at a common CA (= LA_{90}–LA). We demonstrated previously that juniper trees that grew more slowly prior to drought were disproportionately likely to die during or following drought (Polley et al. 2016). Mortality was positively correlated with growth deviation from maximum, calculated by subtracting the basal area increment (BAI) per tree from the BAI value at the 90th percentile of a quantile regression fit to a BAI-CA relationship (BAI_{90}-BAI) across trees (Polley et al. 2016). Growth deviation from maximum was, in turn, linearly correlated to LA deviation from maximum [(BAI_{90}–BAI; cm^2/year) = $5.77 + 0.29 \times (LA_{90}$–LA; m^2); adj. $r^2 = 0.57$, $P < 0.0001$, $n = 58$ trees]. The extreme drought of 2011 killed 87% of sampled Ashe juniper trees for which BAI_{90}–BAI > 16 cm^2/year (Polley et al. 2016). As calculated using the regression equation above, BAI_{90}–BAI > 16 cm^2/year when LA_{90}–LA > 35 m^2. We assigned mortality risk to living juniper individuals for which LA_{90}–LA > 35 m^2. Mortality following the 2011 drought was correlated with the absolute, rather than relative, difference between LA_{90} and LA (Polley et al. 2016). Consequently, we could not assign mortality risk to trees with maximum potential LA (LA_{90}) < 35 m^2 ($\sim$ 7.3 m^2 CA).

Results

The frequency-size distribution (FSD) of Ashe juniper trees at each savanna location was approximately bell-shaped, with peak abundance at intermediate size classes (Fig. 1). Frequency peaked at CA of 20–30 m^2 at both Bend and Temple. Trees were larger on average at Moffat ranch where the peak CA extended between 20 and 50 m^2. Frequency of trees larger than approximately 40 m^2 CA declined precipitously at all sites.

A PLSR with five latent variables accounted for 73% of the variance in LAI of juniper individuals (Fig. 2), with PRESS = 8, equating to 22% of the mean LAI value for the calibration data set (3.74, $n = 53$). Standardized weightings of PLSR coefficients provide insight into which portions of the reflectance spectrum best captured variation in LAI (Fig. 3). LAI was most strongly associated with reflectance in wavebands in the blue (350–400 nm) and near infrared (950–970 and 1030–1060 nm) portions of the spectrum, as indicated by the larger departures of standardized coefficients from the zero line over these spectral ranges.

Maximum values of PLSR-derived estimates of leaf area (LA) were linearly correlated to CA across juniper trees from Temple, Bend, and Moffat

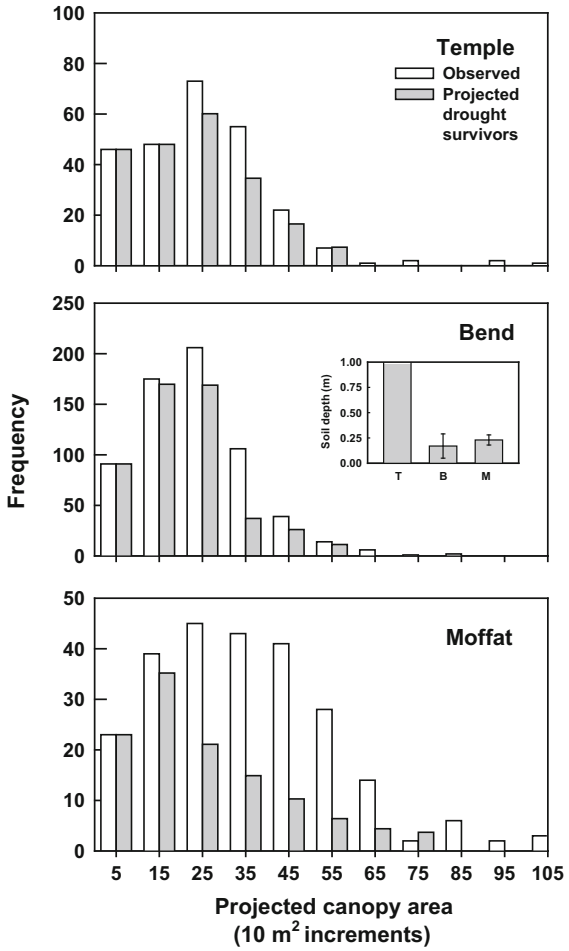

Fig. 1 Frequency-size distribution of living Ashe juniper trees at each of three savanna sites (open bars; n = 257, 640, and 246 trees total for Temple, Bend, and Moffat, respectively) and of trees projected to survive severe drought (filled bars). Based on previous analyses (Polley et al. 2016), we project that severe drought will kill 87% of measured trees in each size class for which the difference between observed leaf area (LA) and the LA of a fully foliated individual of the same size (LA_{90}) exceeds 35 m^2. Size, measured as projected canopy area (CA) per tree, was calculated from manual or remote sensing measurements (n = 240, 162, and 220 remote measurements for Temple, Bend, and Moffatt, respectively). Frequency (number of trees) is plotted at the mid-point of CA bin increments of 10 m^2, beginning for increment 0–10 m^2 CA. Frequency of projected survivors in the largest size class shown per site was calculated for the combined total of all trees in that and larger size classes. Note that scale of the y-axis differs among panels. The insert shows soil depth (m) per site (± SE), measured as the average depth to which a metal rod could be hammered into soil at tree dripline (n = > 15 trees/site). Soil depth exceeded 1 m for all sampled trees at Temple (T), but varied widely among trees growing on soils underlain by fractured limestone at Bend (B) and Moffat (M)

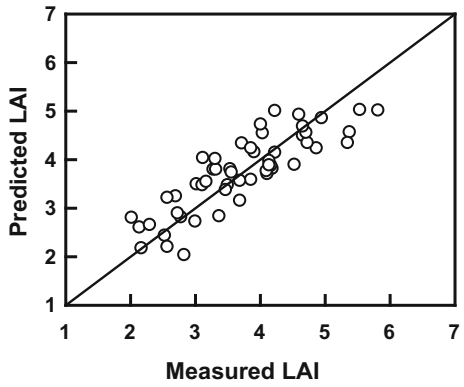

Fig. 2 The relationship between leaf area index (LAI) calculated from measurements of canopy light interception (measured LAI) and LAI predicted from measurements of spectral reflectance using partial least squares regression (PLSR; predicted LAI). PLSR explained 73% of the variance in LAI of juniper individuals (n = 53). The line shows the 1:1 relationship with measured LAI

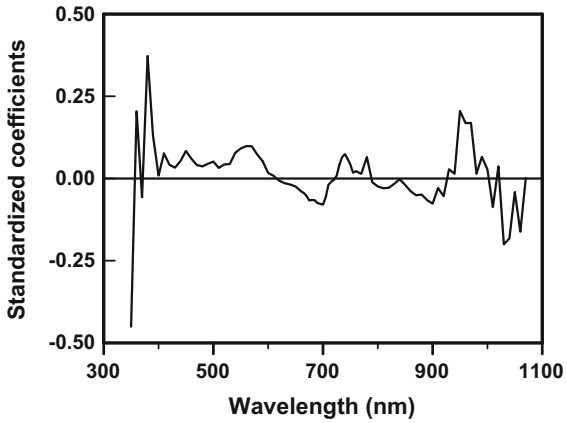

Fig. 3 Standardized weightings of partial least squares regression coefficients from a regression relationship between the measured LAI of juniper individuals and canopy reflectance (n = 53)

combined (Fig. 4, n = 622). For a given CA, LA was 28.6 m^2 smaller on average than the LA derived from a 0.9 regression quantile model fit to the LA versus CA relationship (e.g., LA_{90}–LA = 28.6 m^2). We found previously that most juniper individuals for which LA_{90}–LA exceeded 35 m^2 (87%) died following a severe drought (Polley et al. 2016). LA_{90}–LA exceeded 35 m^2 for 28% of juniper trees sampled at the 3 sites combined.

This index of mortality risk (LA_{90}–LA > 35 m^2) was greatest on average for large than intermediately

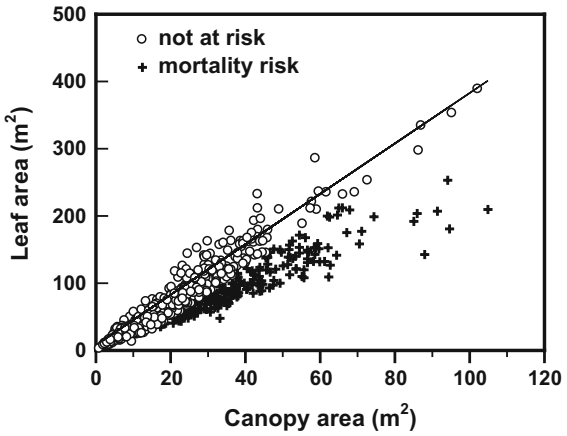

Fig. 4 Leaf area (LA) plotted as a function of projected canopy area (CA) for living Ashe juniper trees in savannas at Temple, Bend, and Moffat, Texas. The solid line is a 0.9 quantile regression fit to the LA–CA relationship (= LA_{90}; $P < 0.0001$, $n = 622$). Symbols are used to distinguish between trees for which LA_{90}–$LA > 35$ m^2 (at risk of drought mortality) versus < 35 m^2 (not at risk)

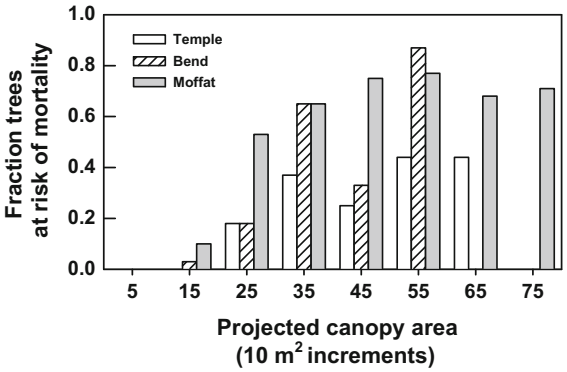

Fig. 5 Fraction of living Ashe juniper trees projected to be at risk of drought mortality as a function of projected canopy area (CA) for each of three savanna sites [$n = 240$, 162, and 220 trees total for Temple (open bars), Bend (hatched bars), and Moffat (closed bars), respectively]. Fractional mortality risk was calculated by dividing the product of 0.87 and the number of trees in each size class for which the difference between observed leaf area (LA) and the LA of a fully foliated individual of the same size (LA_{90}) exceeded 35 m^2 by the total number of trees in each class. 0.87 is the fraction of trees with LA_{90}–$LA > 35$ m^2 that died following severe drought in 2011 (Polley et al. 2016). Mortality risk is plotted at the mid-point of CA bin increments of 10 m^2, beginning at increment 0–10 m^2 CA ($n = 4$–55 trees per CA bin class). Frequencies for the largest size classes shown per site were calculated for the combined total of all trees in that and larger size classes

sized trees, exceeding 40% for trees with CA > 50 m^2 at all sites (Fig. 5). Mortality risk was particularly great among larger trees at Bend and Moffat, where 68–87% of trees with CA > 50 m^2 were judged vulnerable to mortality from severe drought. Mortality risk differed among sites. Risk was least on average on deep soils at Temple and greatest on more shallow soil at Moffat. Risk at the Moffat site exceeded 50% among all trees with CA > 20 m^2.

The number of trees of a given size class that succumb to drought depends on both the frequency of trees in that class and relative vulnerability of similarly sized individuals. As estimated using deviation of canopy foliation from maximum (LA_{90}–LA), the number of trees at risk of mortality at each site is greatest in the most heavily populated size class plus the next 1–2 classes with larger-sized individuals (Fig. 1). Tree frequency peaked at CA = 20–30 m^2 at all sites. The number of at-risk individuals was greatest among trees with CA of 20–40 m^2 (Temple, Bend) or 20–50 m^2 (Moffat).

Discussion

Ecosystem impacts of woody mortality following disturbances depend on both the number and sizes of trees that die. A limited capacity to predict mortality risk of individual trees hinders the capacity to forecast drought effects on population demography and ecosystem functioning. We remotely measured leaf area per unit of canopy area of living individuals of Ashe juniper trees at three savanna sites to characterize the FSD of juniper populations and evaluate mortality risk from drought as a function of tree size. Ashe juniper is a keystone woody species in central Texas, USA, having increased in density in live oak savannas during the last $\sim$ 100 years. We found that abundance was greatest among juniper trees of intermediate size classes at each of three sites. Mortality risk from severe drought exceeded 25% of juniper populations and was highest at a grazed ranch with trees that were larger on average than at other sites. Our results demonstrate the successful use of remote measurements of canopy foliation to link mortality risk from drought to the demography of the emergent juniper population in savannas through properties of individual trees. Results imply that severe drought could kill a large fraction (18–85% depending upon location) of intermediate- to large-sized Ashe juniper trees in central Texas savannas.

The FSD of emergent trees in the juniper populations we studied was approximately bell-shaped with maximum frequency at intermediate trees sizes, typical for tree populations in savannas where emergent individuals are dispersed in a matrix of herbaceous vegetation. This FSD differs from that typical of natural forests where both abundance and mortality rate typically are greatest among juveniles and abundance declines progressively among larger trees (e.g., Coomes et al. 2003). Trees of intermediate size may dominate emergent populations when establishment occurs nearly synchronously following a change in weather or the disturbance regime, as following a favorable weather pattern (e.g., high rainfall) or, for Ashe juniper, the cessation of fire or similar disturbances that preferentially kill small trees (Noel and Fowler 2007; Taylor et al. 2012). One size class of tree may dominate juniper populations for years following episodic establishment, as competition or fire reduces subsequent establishment. Mortality rate eventually increases among the largest and presumably oldest trees to create the approximately bell-shaped FSD. Juniper frequency was high across a wider range of tree sizes at Moffat than Temple or Bend, implying that conditions conducive to juniper establishment and early growth were prolonged at the grazed ranch compared to the other sites.

Our canopy-based estimate of mortality risk for juniper trees was high across study sites, exceeding 25% of all trees sampled. Risk does not indicate outcome. That is, far fewer than 25% of the juniper population may die following drought, even severe drought. Yet, our estimate of mortality risk is similar in magnitude to the observed rate of juniper mortality in central Texas following the 2011 drought. Ashe juniper suffered 27% canopy dieback in the Edwards Plateau region of Texas following this severe drought (Johnson et al. 2018). High mortality risk implies that a recurrence of severe drought or the incidence of other mortality factors that are linked to canopy foliation could substantially reduce the frequency and density of Ashe juniper trees in these savannas.

Larger trees are thought to exert disproportionate control on ecosystem processes (Belsky et al. 1989; Stephenson et al. 2014). Ecosystem-level impacts of tree mortality, therefore, depend partly on the sizes of trees that die (Anderegg et al. 2016; Pfeifer et al. 2011). Drought often kills a disproportionate number of large trees (Bennett et al. 2015; Moore et al. 2016; Mueller et al. 2005). Our analysis indicates that mortality risk is concentrated among juniper trees of intermediate to large size, including the most heavily populated size classes of trees. Heightened risk among dominant size classes implies that drought will have a large impact on the demographic structure of these juniper populations. Drought is an important regulator of tree demographics in savannas generally. Drought, rather than fire, exerts predominant control on tree demographics in semi-arid Australian savanna (e.g., Fensham et al. 2017).

Juniper trees were both larger on average and exhibited the greatest risk of mortality at Moffat among study sites. Size and mortality risk are correlated, as detailed above, but even among similarly sized trees mortality risk usually was greater at Moffat than other sites. It was visually evident that juniper trees typically were more sparsely foliated at Moffat than Bend or Temple. Yet, we observed relatively few dead trees. We infer that the 2011 drought reduced leaf area per unit of CA and slowed growth rather than killed most juniper trees at this site. Plant mortality often represents an end-point response to cumulative impairments of physiological processes (Pedersen 1998). Individuals of tree species that have been growing most slowly are disproportionately predisposed to mortality during drought (Ogle et al. 2000; Suarez et al. 2005). Future drought could, therefore, kill a large fraction of juniper populations that have been weakened by prior stresses.

Ecosystem impacts of woody mortality depend on both the number and size distribution of trees that die. A limited capacity to predict disturbance effects on tree demography impedes forecasts of ecosystem consequences. Methods that link disturbance effects to properties of individual trees may ultimately be required to more fully characterize shifts in the population demography of trees and ecosystem functioning. Heightened mortality risk in Ashe juniper is linked to slow growth which, in turn, is linked to reduced LA (Polley et al. 2016). Carnicer et al. (2011) also reported correlations among water deficit, tree foliation, and mortality rates in drier portions of the ranges of woody species. We used established correlations among leaf area, growth rate, and mortality to demonstrate how remote measurements of the LAI and CA of living individuals can be used to predict drought vulnerability of emergent individuals of Ashe juniper. Other approaches to discern the LA and sizes

of individual trees (e.g., Colgan et al. 2012) might similarly be used to link disturbance effects on individuals to population dynamics of keystone woody species and, ultimately, to ecosystem functioning.

Acknowledgements Assistance from Chris Kolodziejczyk and Katherine Jones was critical. We are indebted to Texas Parks and Wildlife staff at Colorado Bend State Park and Ms. Lois Reiter for their gracious cooperation. This project was funded under a Grant from USDA-AFRI (#2012-00857). Mention of trade names or commercial products does not imply endorsement by the US Department of Agriculture. USDA is an equal opportunity provider and employer.

References

Adams HD, Luce CH, Breshears DD, Allen CD, Weiler M, Hale VC, Smith AMS, Huxman TE (2012) Ecohydrological consequences of drought- and infestation-triggered tree die-off: insights and hypotheses. Ecohydrology 5:145–159

Allen CD, Macalady AK, Chenchouni H, Bachelet D, McDowell N, Vennetier M, Kitzberger T, Rigling A, Breshears DD, Hogg EH, Gonzalez P, Fensham R, Zhang Z, Castro J, Demidova N, Lim J-H, Allard G, Running SW, Semerci A, Cobb N (2010) A global overview of drought and heat-induced tree mortality reveals emerging climate change risks for forests. For Ecol Manage 259:660–684. https://doi.org/10.1016/j.foreco.2009.09.001

Allred BW, Fuhlendorf SD, Smeins FE, Taylor CA (2012) Herbivore species and grazing intensity regulated community composition and an encroaching woody plant in semi-arid rangeland. Basic Appl Ecol 13:149–158

Anderegg WRL, Martinez-Vilalta J, Cailleret M, Camarero JJ, Ewers BE, Galbraith D, Gessler A, Grote R, Huang C, Levick SR, Powell TL, Rowland L, Sánchez-Salguero R, Trotsiuk V (2016) When a tree dies in the forest: scaling climate-driven tree mortality to ecosystem water and carbon fluxes. Ecosystems 19:1133–1147

Belsky AJ, Amundson RG, Duxbury JM, Riha SJ, Ali AR, Mwonga SM (1989) The effects of trees on their physical, chemical, and biological environments in a semi-arid savanna in Kenya. J Appl Ecol 26:1005–1024

Bennett AC, McDowell NG, Allen CD, Anderson-Teixeira KJ (2015) Larger trees suffer most during drought in forests worldwide. Nat Plants. https://doi.org/10.1038/nplants.2015.139

Cade BS, Noon BR (2003) A gentle introduction to quantile regression for ecologists. Front Ecol Environ 1:412–420

Carnicer J, Coll M, Ninyerola M, Pons X, Sánchez G, Peñuelas J (2011) Widespread crown condition decline, food web disruption, and amplified tree mortality with increased climate change-type drought. Proc Natl Acad Sci USA 108:1474–1478

Colgan MS, Baldeck CA, Féret J-B, Asner GP (2012) Mapping savanna tree species at ecosystem scales using support vector machine classification and BRDF correction on airborne hyperspectral and LiDAR data. Remote Sens-Basel 4:3462–3480

Coomes DA, Duncan RP, Allen RB, Truscott J (2003) Disturbances prevent stem size-density distributions in natural forests from following scaling relationships. Ecol Lett 6:980–989

Feilhauer H, Asner GP, Martin RE, Schmidtlein S (2010) Brightness-normalized partial least squares regression for hyperspectral data. J Quant Spectrosc Radiat Transfer 111:1947–1957

Fensham RJ, Freeman ME, Laffineur B, Macdermott H, Prior LD, Werner PA (2017) Variable rainfall has a greater effect than fire on the demography of the dominant tree in a semi-arid Eucalyptus savanna. Austral Ecol 42:772–782

Floyd ML, Clifford M, Cobb NS, Hanna D, Delph R, Ford P, Turner D (2009) Relationship of stand characteristics to drought-induced mortality in three Southwestern piñon-juniper woodlands. Ecol Appl 19:1223–1230

Guardiola-Claramonte M, Troch PA, Breshears DD, Huxman TE, Switanek MB, Durcik M, Cobb NS (2011) Decreased streamflow in semi-arid basins following drought-induced tree die-off: a counter-intuitive and indirect climate impact on hydrology. J Hydrol 406:225–233. https://doi.org/10.1016/j.jhydrol.2011.06.017

Hoerling M, Kumar A, Dole R, Nielsen-Gammon JW, Eischeid J, Perlwitz J, Quan X-W, Zhang T, Pegion P, Chen M (2013) Anatomy of an extreme event. J Climate 26:2811–2832. https://doi.org/10.1175/JCLI-D-12-00270.1

Huang C, Asner GP, Barger NN, Neff JC, Floyd ML (2010) Regional aboveground live carbon losses due to drought-induced tree dieback in piñon-juniper ecosystems. Remote Sens Environ 114:1471–1479

IPCC (2013) Climate change 2013: The physical science basis. Working Group I contribution to the Fifth assessment report of the Intergovernmental Panel on climate change. Cambridge University Press, Cambridge

Johnson DM, Domec J-C, Berry ZC, Schwantes AM, McCulloh KA, Woodruff DR, Polley HW, Wortemann R, Swenson JJ, Mackay DS, McDowell NG, Jackson RB (2018) Co-occurring woody species have diverse hydraulic strategies and mortality rates during an extreme drought. Plant Cell Environ 41:576–588

Michaelian M, Hogg EH, Hall RJ, Arsenault E (2011) Massive mortality of aspen following severe drought along the southern edge of the Canadian boreal forest. Glob Change Biol 17:2084–2094. https://doi.org/10.1111/j.1365-2486.2010.02357.x

Moore GW, Edgar CB, Vogel JG, Washington-Allen RA, March RG, Zehnder R (2016) Tree mortality from an exceptional drought spanning mesic to semiarid ecoregions. Ecol Appl 26:602–611

Mueller RC, Scudder CM, Porter ME, Trotter RT III, Gehring CA, Whitham TG (2005) Differential tree mortality in response to severe drought: evidence for long-term vegetation shifts. J Ecol 93:1085–1093

Noel JM, Fowler NL (2007) Effects of fire and neighboring trees on Ashe juniper. Rangel Ecol Manage 60:596–603

Ogle K, Whitham TG, Cobb HS (2000) Tree-ring variation in pinyon predicts likelihood of death following severe drought. Ecology 81:3237–3243

Pedersen BS (1998) The role of stress in the mortality of midwestern oaks as indicated by growth prior to death. Ecology 79:79–93

Peng CH, Ma ZH, Lei XD, Zhu QA, Chen H, Wang WF, Liu SR, Li WZ, Fang XQ, Zhou XL (2011) A drought induced pervasive increase in tree mortality across Canada's boreal forests. Nat Clim Change 1:467–471

Pfeifer EM, Hicke JA, Meddens AJH (2011) Observations and modeling of aboveground tree carbon stocks and fluxes following a bark beetle outbreak in the western United States. Glob Change Biol 17:339–350

Polley HW, Johnson DM, Jackson RB (2016) Canopy foliation and area as predictors of mortality risk from episodic drought for individual trees of Ashe juniper. Plant Ecol 217:1105–1114

Riskind DH, Diamond DD (1988) An introduction to environments and vegetation. In: Amos BB, Gehlbach FR (eds) Edwards Plateau vegetation—plant ecological studies in central Texas. Baylor University Press, Waco, pp 1–15

Schwantes AM, Swenson JJ, Jackson RB (2016) Quantifying drought-induced tree mortality in the open canopy woods of central Texas. Remote Sens Environ 181:54–64

Schwantes AM, Swenson JJ, González-Roglich M, Johnson DM, Domec J-C, Jackson RB (2017) Measuring canopy loss and climatic thresholds from an extreme drought along a 5-fold precipitation gradient across Texas. Glob Change Biol 23:5120–5135. https://doi.org/10.1111/gcb.13775

Schwinning S (2008) The water relations of two evergreen tree species in a karst savanna. Oecologia 158:373–383

Smeins FE, Merrill LB (1988) Long-term change in a semi-arid grassland. In: Amos BB, Gehlbach FR (eds) Edwards plateau vegetation—plant ecological studies in central Texas. Baylor University Press, Waco, pp 101–114

Stephenson NL, Das AJ, Condit R, Russo SE, Baker PJ, Beckman NG, Coomes DA, Lines ER, Morris WK, Rüger N et al (2014) Rate of tree carbon accumulation increases continuously with tree size. Nature 507:90–93

Suarez ML, Ghermandi L, Kitzberger T (2005) Factors predisposing episodic drought-induced tree mortality in Nothofagus: site, climatic sensitivity, and growth trends. J Ecol 92:954–966

Taucer PI, Munster CL, Wilcox BP, Owens MK, Mohanty BP (2008) Large-scale rainfall simulation experiments on juniper rangelands. T ASABE 51:1951–1961

Taylor CA Jr, Twidwell D, Garza NE, Rosser C, Hoffman JK, Brooks TD (2012) Long-term effects of fire, livestock herbivory removal, and weather variability in Texas semiarid savanna. Rangel Ecol Manage 65:21–30

Trenberth KE, Dai A, van der Schrier G, Jones PD, Barichivich J, Briffa KR, Sheffield J (2014) Global warming and changes in drought. Nature Clim Change 4:17–22

Wold S, Ruhe A, Wold H, Dunn WJ III (1984) The collinearity problem in linear regression. The partial least squares (PLS) approach to generalized inverses. SIAM J Sci Stat Comput 5:735–743